

EFFECT OF CROSSLINK DENSITY ON THE
CREEP BEHAVIOR OF NATURAL RUBBER VULCANIZATES^a

Donald J. Plazek

Mellon Institute
Pittsburgh, Pa. 15213

FACILITY FORM 602

<u>N66-14531</u> (ACCESSION NUMBER)	<u>1</u> (THRU)
<u>37</u> (PAGES)	<u>18</u> (CODE)
<u>CR69896</u> (NASA CR OR TMX OR AD NUMBER)	<u>18</u> (CATEGORY)

GPO PRICE \$ _____

CFSTI PRICE(S) \$ _____

Hard copy (HC) 2.00

Microfiche (MF) .50

ff 653 July 65

^a This paper was presented at the 36th Annual Meeting of the Society of Rheology which was held at Case Institute of Technology, Cleveland, Ohio, October 25-27, 1965.

NBSA

N66-14531

ABSTRACT

14531
Torsional creep measurements on four natural rubber vulcanizates, crosslinked to different degrees, were carried out in the temperature range -50°C to 90°C . This investigation complements the studies on identical samples of the stress relaxation behavior by Chasset and Thirion and of the dynamic mechanical response by Ferry, Mancke, Maekawa, Oyanagi, and Dickie. The creep measurements being reported are shown to be in agreement with the stress relaxation results. In addition to the usual temperature reduction, a superposed curve was obtained using the apparent molecular weight between crosslinks, M_c , as a reduction variable. The variation in viscoelastic response with crosslink density is interpreted as a restrictive action of the chemical crosslinks on the transient entanglement network.

Author

INTRODUCTION

The viscoelastic behavior of crosslinked elastomers in the transition from glasslike to rubberlike behavior has been frequently studied,¹⁻⁵ and a number of the investigations have extended well into the rubbery region of response.⁶⁻¹⁰ In this latter region the lack of equilibrium behavior of polymer networks has been observed as continuing stress decay at constant strain or increasing deformation under constant load. Under sinusoidal deformation a low but persistent loss is observed even at the lowest frequencies of measurement. However, little progress has been made in establishing the systematic phenomenological patterns of behavior which are characteristic of these materials at long times, much less in understanding the molecular processes responsible for the lack of time-independent response.

Recently a series of natural rubber samples crosslinked to various degrees was prepared in the laboratory of Dr. Pierre Thirion, Institut Francais du Caoutchouc, Paris. Careful stress relaxation measurements on this series made by Chasset and Thirion¹¹ clearly showed that the degree of crosslinking is the dominating variable for the response in the long time domain. A study was first made¹² at temperatures between 65° and 100°C where thermal degradation is the principal contributor to stress decay after the first day or two following the application of strain to the rubber. With the resulting information on the kinetics of degradation it was possible to predict the onset of a measurable contribution by degradation to the relaxation. Measurements were confined to times where the

response was entirely viscoelastic in the subsequent study.

Identical samples at five different crosslinking levels were sent to the laboratory of Professor John D. Ferry, University of Wisconsin, Madison, where R. G. Mancke, E. Maekawa, Y. Oyanagi and R. A. Dickie¹³ assisted in characterizing the dynamic mechanical properties in the region of time scale extending from the glasslike to rubberlike transition to that covered by the stress relaxation measurements.

Shear creep compliance, $J(t)$, results are being reported here on four samples of this natural rubber series that have generously been provided to us by Dr. Thirion. These complementary results encompass the entire range of reduced time covered in the other two investigations and help give a unified picture of the effect of crosslinking on the viscoelastic response of crosslinked polymers.

EXPERIMENTAL

The natural rubber, NR, samples were prepared from smoked sheet rubber that had a low content of inorganic impurities. 3.5% of the cross-linking agent, dicumyl peroxide (DCP) was used and the vulcanization time at 135°C was varied to obtain the different degrees of crosslinking, see Table I. The equilibrium swelling in benzene at room temperature was determined to insure that our samples had not changed since their preparation. Using the values of the volume fraction of rubber in the swollen samples,

v_2 , in the Flory-Rehner equation,¹⁴
$$M_c = \frac{\rho V_o (v_2^{1/3} - \frac{1}{2} v_2)}{-\ln(1-v_2) - v_2 - \mu v_2^2}$$
, the

apparent effective molecular weight between crosslinks, M_c , was calculated. V_o is the solvent molar volume, ρ is the density of the dry rubber and $\mu = 0.444$ is the natural rubber-benzene polymer-solvent interaction coefficient determined by Chasset and Thirion. Densities were determined by means of flotation in ethanol-water mixtures and cubic thermal expansion coefficients, α , from length measurements with a traveling microscope. The results for α on the NR samples scattered between 6.2 and $5.7 \times 10^{-4} \text{ } ^\circ\text{C}^{-1}$ and an average of 6.0×10^{-4} was used. The values of ρ and v_2 are given in Table I along with the resultant M_c 's, which agree within experimental error with those reported by Thirion and Chasset.¹¹ The swelling medium was reagent grade thiophene-free benzene (J. T. Baker Chemical Co., Phillipsburg, N. J.).

Table I
 Characteristics of the Rubber Vulcanizates

Vulcanizate	Curing time (min.)	$\rho(30^\circ)$ g/cm ³	v_2^a	Sol fraction $\times 100$	M_c^b	M_c^c
F	20	0.9086	0.129 ₁	4.6	20,500	20,000
G	30	---	---	---	---	14,800
H	40	0.9086	0.167 ₃	3.6	11,200	11,400
I	75	0.9092	0.196 ₁	3.3	7,400	7,600
J	150	0.9099	0.224 ₁	3.0	5,200	5,400

a, swelling medium is benzene; b, from swelling in this study; c, from swelling ref. 11.

Most of the shear creep compliance results being reported were obtained using a torsion instrument¹⁵ with a rotor which floated in an extremely low vapor pressure liquid (tri-m-tolyl phosphate). Measurements on the rubbers were made both with the original torque-producing device, a modified pair of wattmeter drive units, and with a later-developed drag cup motor for precise torque production. The field coils of the motor produce a rotating magnetic field which induces a drag torque on an essentially static aluminum cup that resides in an annulus air gap. The same kind of motor is used in the other creep instrument used in this study. In this latter instrument a magnetic bearing is used to support the rotor and the sample atmosphere can be controlled. In addition to checking many of the measurements made in the float instrument this second apparatus, with its wider temperature range, was used to obtain results at temperatures down to -50°C . The specimens measured were right circular cylinders about 0.4 cm. in diameter and 0.5 cm. high. Maximum strains of about 1% were experienced by the specimens.

RESULTS

The four natural rubber samples F, H, I, and J were each measured in the float torsional creep apparatus at 5 or 6 temperatures in the range 0° to 90°C. Most of the shear creep compliance curves, $J(t)$, cm^2/dyne , obtained on samples F and I are presented logarithmically in Fig. 1 as a function of logarithmic time (where the time is expressed in seconds). $J_p(t) = J(t) \frac{T_0}{T_0 \rho_0}$, where T is the absolute temperature, has been plotted to account for the entropic nature of the response.¹⁶ Note change in scale F to I. Several of the problems encountered in the investigation are illustrated in these data.

The effect of crystallization during a creep run can be easily seen in the 1°C curve of sample F as positive curvature following the point of inflection at $\log t = 4.5$. Such an increase in the derivative $d \log J(t)/d \log t$ need not necessarily reflect additional crystallization occurring during the creep run but could indicate concurrent thermal degradation or the onset of an actual additional viscoelastic dispersion. However, since the melting point, T_m , of natural rubber is 28°C,¹⁷ and since its depression by moderate crosslinking is slight¹⁸ it was realized that some crystallization might occur at the lower temperatures of measurement. Below 30°C noticeable thermal degradation does not occur during periods of one to 10 hours,¹² so an isothermal drop in the compliance curve with time was concluded to indicate a growing degree of crystallinity. The compliance decrease was measured either by carrying out successive short creep runs (10 seconds) with the sample otherwise in an unloaded condition, or by removing the torque periodically for 10 seconds during a prolonged creep run. Such

intermittent checks do not affect the creep response measurably for longer than a few minutes, and were also used after the first hour of creep at higher temperatures to detect the presence of thermal degradation. Since the rate of creep was small for most of the measurements following shorter runs, the first 10 seconds of the recovery provide an identical check on the level of response. Check runs at 30°C preceding and following most measurements were also used to keep track of the sample stability. In spite of the enhancement of the deformation caused by the occurrence of crystallization, the compliance level, as measured by the recovery portion of the run and a subsequent short check run, fell an appreciable 16% during the 3-day run. The enhancement suggests that even at the low stress imposed on the sample (2×10^4 dynes/cm² maximum) the orientation of the chains in the crystallites formed was biased in the direction of the applied stress. Subsequent heating above the melting point restored the original compliance level, thereby confirming the above conclusions. Since we found, in agreement with previous work,^{19,20} that the compliance decrease caused by the early stages of crystallization is linear in time, a one percent change was present after the sample was at temperature for three hours. One can therefore confidently accept the results up to 10^4 seconds at 1°C. The rate of crystallization diminishes appreciably with increasing crosslinking,¹⁸ so other members of the NR series are less affected.

Checks during and after the 3-day run at 30°C indicated a one percent decrease in compliance by the end of the run. Nothing was observed in the rest of our measurements to indicate an additional viscoelastic

dispersion in this region and four other samples^a consistently yielded an increase in compliance level during and after measurement when degradation occurred at the higher temperatures, 40 to 90°C. We are left with the conclusion that the abrupt increase in $d^2 \log J(t)/d \log t^2$ at 30°C was caused by a slight amount of crystallization which was induced by the applied stress.

Since for the NR samples thermal degradation inevitably led to an increase in compliance level, reflecting a decrease in the concentration of effective network chains, it can be concluded that the free radicals formed upon chain scission were terminated and became loose-ended chains. Our measurements were carried out in air. Since similar measurements by Gent²¹ which focused on the degradation-enhanced creep (secondary creep) showed a marked decrease in the secondary creep when carried out in vacuum, it is reasonable that the free radicals react with oxygen. The 40 and 60° curves for I, shown in Figure 1 show an appreciable secondary creep contribution to the measured compliance beyond $\log t = 3$.

The very small slopes exhibited by the $\log J_p(t)$ curves complicated the reduction procedure slightly. Relatively small errors in sample coefficient or instrument parameter values can cause enormous errors in the temperature shift factor, a_T ,²² or make reduction completely impossible. We have therefore matched the curvature of runs at different temperatures to achieve reduction and allowed ourselves the freedom of applying the necessary vertical shifts to achieve superposition. The logarithms of

^a A fifth sample, K, was measured, but since the swelling and the creep behavior differed very little from F the results are not being reported here. A 20-hour creep measurement at 40°C on this vulcanizate showed no abrupt increase in $d^2 \log J(t)/d \log t^2$ and no change in compliance level, thereby arguing for no degradation in F at 30°C.

the a_T and empirical vertical shift factors, $\Delta \log J(T)$, used are presented in Table II. For all of the measurements taken above 0°C the $\Delta \log J(T)$ shifts are within our ± 1 percent repeatability after a temperature cycle. We believe our results to be accurate within about 3 percent and our precision within a run is about 1/4 percent. In addition to thermal degradation, occasional crystallization, sample coefficient errors, and the uncertainty in the instrument parameters (some of which have been considerably reduced since this investigation began) we believe our precision was limited by a dependence of the shear compliance on the slight axial compression (ca. 2%) on the sample.²³ In Figure 2 the resulting reduced $\log J_p(t)$ curves (reference temperature, $T_o = 30^\circ\text{C}$) are shown for the samples NR-F, H, I, and J. It is clear that the degree of crosslinking has a pronounced effect on the percentage increase of creep observed in this region. In fact, the amount of creep exhibited by F is about 10 fold that displayed by J. The dash lines in Figure 2 were calculated from the elongational stress relaxation results of Chasset and Thirion. Force values divided by the unstressed sample cross-sectional areas,^{11,24} $\sigma(t)$, were reported. The derived quantity represented by the dashed lines is $\frac{\sin m \pi}{m \pi} \left(\frac{\lambda - \lambda^{-2}}{\sigma(t)} \right)$,²⁵ where $m = d \log \sigma(t) / d \log t$ and λ , the elongation ratio = 1.50. Extrapolating isochronal values of $\sigma/(\lambda - \lambda^{-2})$ from Chasset and Thirion's measurements at different elongation ratios to $\lambda = 1.0$ an increase of $9.5 \pm 1.0\%$ is obtained. Assuming that Poisson's ratio, μ , is 1/2, to a good degree of approximation $\lim_{\lambda \rightarrow 1} \frac{\sin m \pi}{m \pi} \left(\frac{\lambda - \lambda^{-2}}{\sigma(t)} \right)$ should be equal to $J(t)$. The actual percentage differences obtained

Table II

Derived Parameters of the Rubber Vulcanizates

Vulcanizate	T°C	log a _T	Δ log J(t)	log J _e	log $\frac{J_e(F)^a}{J_e(x)}$	log $\frac{J_e(F)^b}{J_e(x)}$	log a _x
F	1	1.34	0.010				
	10	0.85	0.000				
	20	0.41	0.000				
	30	0	0.000	-6.227	0	0	0
	40	-0.18	-0.004				
	60	-0.71	-0.010				
G	30	---	---	-6.357	0.130	0.132	-2.48
H	0.7	1.42	-0.004 ₅				
	10	0.73	-0.003 ₅				
	20	0.33	-0.003				
	30	0	0.000	-6.460	0.233	0.231	-4.15
	40	-0.32	-0.003				
	60	-0.76	0.000				
I	1	1.20	0.0014				
	10	0.71	0.0016				
	20	0.32	0.0000				
	30	0	0.0000	-6.606	0.379	0.382	-6.76
	40	-0.24	0.0012				
	60	-0.62	0.0010				
J	-49.8	6.52	0.0115				
	-35.5	4.57	-0.0006				
	-23.7	3.40	0.0090				
	-10.4	2.20	0.0000				
	1.0	1.27	-0.0063				
	10	0.63	-0.0040				
	20	0.20	-0.0025				
	30	0	0.0000	-6.717	0.490	0.484	-9.94
	40	-0.33	0.0005				
	60	-0.70	0.0025				
90	-1.00	0.0061					

a, this study; b, from reference 11 using extrapolated not averaged values.

between the $J_p(t)$ and $\lambda = 1.50$ curves, as seen in Fig. 2, are F, 9.1; H, 8.6; I, 7.2, and J, 7.9%. The agreement is within the estimate of our absolute accuracy of 3% and it is concluded that our shear creep compliance results are in complete accord with the elongational stress relaxation results of Chasset and Thirion. The reduced $\log J_p(t)$ curves for samples I and J are shown plotted in Fig. 3 with an appropriately expanded ordinate scale where the degree of scatter and the contribution of thermal degradation can be more readily assessed.

M_c reduction

It is widely acknowledged that the equilibrium response of an elastomer is largely independent of the chemical character of the polymeric chains making up the molecular network. The statistical mechanical theory of rubberlike elasticity indicates that only the number of effective molecular chains per cm^3 is important.²⁶ A small effect for dry rubbers is to be expected if the average chain end to end distance is temperature dependent;^{27,28} and indirectly the chemical character of the polymer has an effect on the concentration of effective chains through the determination of the degree of entanglement present. We would like to propose here that within a constant factor which is related to the average monomeric friction coefficient the approach to mechanical equilibrium of an elastomer is insensitive to its chemical character. In addition it is suggested that the terminal region of the retardation spectrum of an elastomer has one characteristic shape regardless of the degree of crosslinking.[†] Based

[†] It appears reasonable that future measurements may demand that the above statements apply only to randomly crosslinked flexible polymers.

on these propositions it should be possible to construct a universal curve with the creep compliance data shown in Fig. 2. By applying a vertical shift to the curves representing the response of samples H, I, and J, which is presumed to be only a function of the equilibrium shear creep compliance, J_e , and a horizontal shift along the time axis a reduced curve relative to the response of the reference sample F can be constructed. The overlapping portions of the $\log J_p(t)$ curves were found to match in shape within experimental error. Such an empirical shifting procedure was applied with the result being shown in Fig. 4 where

$$\log J_x(t/a_x) = \log J_e(M_c) + \log \frac{J_e(20,300)}{J_e(M_c)} + \log \psi_x(t/a_x).$$

$\psi_x(t)$ is a normalized terminal retardation function, $\lim_{t \rightarrow \infty} \psi_x(t) = 1$. The value for $J_e(20,300)$, that for reference sample F, was taken to be one percent greater than the final level reached by the $J_x(t)$ curve. A linear extrapolation of the $\log L_2(\tau)$, the logarithm of the second approximation to the retardation spectrum,^{22,29} which is also shown in Fig. 4 yields an additional contribution to the compliance of slightly greater than one percent. We believe such an extrapolation results in a maximum estimate of the remaining unobtained creep deformation. The values of the vertical shift employed in obtaining the universal creep curve, $\log \frac{J_e(20,300)}{J_e(M_c)} \equiv \log \frac{J_e(F)}{J_e(x)}$, are compared with those obtained from the mathematical extrapolation procedure employed by Chasset and Thirion in Table II. The excellent agreement is evidence indicating that the graphical reduction

procedure is allowable within the precision of both sets of data. The $\log \frac{J_e(20,300)}{J_e(M_c)}$ values are simply subtracted from the $\log J_e(20,300)$ value of -6.227 to obtain values for the samples at higher crosslinking density. Smoothed values of $\log \psi_x(t)$ are presented in Table III.

The required time axis shifts, $\log a_x$, for superposition of the $\log J_p(t)$ curves are also given in Table II and are shown plotted against $\log M_c$ in Fig. 5. The filled circles on the natural rubber, NR, curve reflect values of M_c calculated from our swelling results and all the open circles from swelling measurements of Chasset and Thirion.¹¹ The $\log a_x$ values shown for the styrene-butadiene rubber, (23.5/76.5) SBR, series of samples were obtained by converting the elongational stress relaxation results of Chasset and Thirion²⁴ to shear creep compliance curves and superposing them on the curve shown in Fig. 4. At present the meaning of the power relationship expressed by the straight lines seen in Fig. 5 is not known, but the fact that within experimental scatter both the NR and SBR lines have the same slope, 15.4, is clear-cut evidence that the form of the $\log J_x(t/a_x)$ curve is the same for these rubbers of highly different chemical structure. It is believed that the displacement of the lines on the $\log a_x$ axis is a measure of the relative average monomeric friction coefficient, ζ_0 . Catsiff and Tobolsky⁷ have compared the stress relaxation behavior of a similar SBR rubber (25/75) to that of a natural rubber sample and found in the region of time scale where monomeric friction coefficients are usually calculated²² that the SBR primary transition is located at longer times by about 2 logarithmic decades. The displacement on the $\log a_x$ axis of the lines in Figure 5 is approximately 3 logarithmic decades.

Table III

Smoothed Normalized Terminal Retardation Function, $\psi_x(t)$
 Position on Time Scale Is That of NR-F

$\log t/a_x$	$\log \psi_x(t)$	$\log t/a_x$	$\log \psi_x(t)$
-1	-0.2315	7	-0.0355
0	-0.1906	8	-0.0277
1	-0.1578	9	-0.0214
2	-0.1286	10	-0.0163
3	-0.1039	11	-0.0122
4	-0.0821	12	-0.0086
5	-0.0606	13	-0.0058
6	-0.0472	14	-0.0040

At the present then it can be said that the enhancement of ζ_0 by entanglements is roughly similar for different polymers. In addition, since many polymers have a $\log \zeta_0$ at T_g in the neighborhood of 4.0^{22} the relative position of lines for rubbers of different chemical structure in Figure 5 should reflect relative values of their T_g 's. Focusing on NR and SBR rubbers with the same M_c 's it can be seen that $\log a_x$ for the SBR rubber is less negative. This means that the SBR rubber is creeping at a relatively greater rate, or in other words it is further from equilibrium. One would therefore conclude that its T_g is higher. A reasonable T_g for a SBR rubber with 23.5% styrene is about -55°C ³⁰ which would place it about 20°C higher than the T_g for natural rubber. More comparisons are in order to check the propositions made here.

Extent of the terminal creep.

The above arguments make clear the need to relate the terminal creep region to the principal peak in L since only relative to it can one measure the breadth of that part of the spectrum contributing to creep in the rubbery plateau. An attempt was therefore made to obtain creep measurements on samples F and J at lower temperatures (i.e., at short equivalent times). Trouble was expected from crystallization so J, the slower crystallizing sample, was measured first. To minimize the amount of crystallization that would occur, rapid cooling past the temperature of fastest crystal growth (ca. -20°C)¹⁸ to -50°C was carried out by immersing the sample chamber of our instrument in a container of dry ice. The sequence of runs on the two samples was: J; 30.0, -49.8 , -23.7 , 30.0,

-35.5, -10.4, and 30.0°C: F; 30.0, -49.8, -35.5, -24.5, -10.2, and 30.0°C. As can be seen by the small necessary vertical shifts for the runs on J, see Table II, negligible crystallization was present throughout the series. The temperature reduced results which extend at short times into the beginning of the primary transition region are shown in Fig. 6. However, it is clear from the low original positions of the low temperature curves for sample F (the dotted lines) that some crystallization occurred during cooling and even greater amounts while sitting near the temperature of fastest crystallization. The positions of these curves on the time scale were determined using the $\log a_T$ shift factors determined from the measurements on J. A slight amount of error is thereby introduced since the different degree of crosslinking necessarily means that the T_g 's are somewhat different and hence also the temperature dependences. It appears as judged by their shapes that negligible crystallization occurred during the 1000 second creep runs at -24.5° and -10.2°C. Furthermore, one can conclude that the degree of crystallinity present during the runs was so small that the form of the response was unaltered. Since the combined runs at -49.8 and -35.5 came close to meeting the reduced curve obtained above 0°C, only they were shifted vertically to the proper position. The solid lines between $\log t/a_T = -1.0$ and 5.0 are the same curves as displayed in Fig. 2 and the dashed lines are the appropriately positioned $\log J_x(t/a_x)$ curves. It can be seen that the $\log J_p(t)$ curve for J significantly departs from the universal curve at $\log t/a_T \simeq -2$. It is evident that the proximity of the primary transition requires such a departure.

Temperature Dependence.

The temperature dependent shift factors, $\log a_T$, for F, H, and J determined between 0 and 90°C are shown in Fig. 7 along with the lower temperature values for J. The universal form of the WLF equation³¹

$$\log a_T = -8.86(T-T_s)/[101.6 + T - T_s]$$

with a $T_s = -21$ ² is drawn in Fig. 7, shifted to a reference temperature of 30°C. The data fall within experimental error on the curve up to 130°C above T_g . This range is more than is usually expected, but we wish to make clear that all of the values of $\log a_T$ determined above 0°C are to be considered relatively unreliable because of the small slopes observed in the primary data.

Retardation Spectra.

The retardation spectrum, L , cm^2/dyne , for all of the reduced data was calculated using the second approximation method of Williams and Ferry, which was adapted to creep by Stern.^{22,29} Several curves were also treated with Leaderman's expression²⁵ with a resulting excellent agreement. The retardation spectra, which reflect all of the information contained in the original data are plotted logarithmically in Fig. 8 as a function of the logarithm of the reduced retardation time, τ_r . The part of the spectrum of F that is presented covers a sizable range of 21 logarithmic decades of reduced time. The dashed line reflects the portion obtained

from the M_c reduction. The extent of the slowly diminishing spectrum shows clearly why many attempts to reach equilibrium deformations in elastomers have failed. To come within one percent of equilibrium in F, assuming no chemical degradation, would take over a million years at 30°C. Those familiar with calculations of spectra will appreciate that the scatter is not abnormal and that within experimental error the shapes of the spectra for H, I, and J beyond $\log \tau_r = 0$ are the same as those parts of F to which the compliance curves of the three respectively contributed. The apparent independence of the form of L to the degree of crosslinking and chemical character indicates that the kinetics of the approach to equilibrium deformation in creep or equilibrium stress in stress relaxation is solely a function of the distance from that equilibrium.

In other reduction schemes shifts of curves along the time axis reflect a difference in average friction coefficient in the original and reduced states. Such is not the case with the M_c reduction. There is certainly very little difference in the terminal region friction coefficients of the differently crosslinked NR samples. We interpret the picture presented in Fig. 8 to indicate that the principal viscoelastic effect of the chemical crosslinks is to eliminate retardation mechanisms arising from non-affine motions or adjustments of the chain entanglements. The attrition of the longest retardation mechanisms is greater resulting in the apparent time axis shift, $\log a_x$. Since both the chain lengths between crosslinks and entanglements have random distributions, as the average chain length between crosslinks approaches the average entanglement length the longest chains between entanglements will be eliminated

from transient load bearing in greater numbers than short chains. If we think of the transient entanglement network and the permanent crosslink network as being interpenetrating, the above point becomes clear.

Parts of molecular chains that are incorporated into the permanent network, by having no entanglements between crosslinks, cannot participate in the long time processes. This picture also demands that as the crosslink density increases the entanglements are more effectively trapped into permanent load bearing. Therefore the efficacy of an entanglement should be greater than at a low crosslink density where time dependent adjustments of the entanglement junctures will lead with greater probability to a transfer of load to nearby chains which are fixed by permanent crosslinks. In view of the viscoelastic response observed at varying crosslink density we cannot accept the assumption of Bueche³² and Mullins³³ that all of the entanglements present in the rubber precursor are equally effective in producing load-bearing chains as are crosslinks. The fact that Mullins deduces what appears to be an unusually high value for M_e , the molecular weight between entanglements in the infinitely long natural rubber precursor (14,000), is evidence that entanglements are less effective than crosslinks. Since we did not have the precursor to our natural rubber samples, creep measurements were made on an uncrosslinked high cis content synthetic cis-isoprene sample.^a An M_e of 6400 was obtained from the Andrade intercept,³⁴ $J_A = \frac{M_c}{\rho RT}$. Other literature values²² obtained from the more arbitrary points of inflection in viscoelastic curves of natural rubber are: 5000, $G'(\omega)$; 6800, $G'(\omega)$; and 8200, $J(t)$. The above

^a This sample was generously supplied to us by Dr. Edward Collins of the B. F. Goodrich Development Center, Avon Lake, Ohio.

conclusions drawn from this study agree in large part with those of Maekawa, Mancke, and Ferry which were deduced from their study on polybutadiene rubbers.³⁶

If the number of crosslinks introduced in an originally linear chain sample is insufficient to produce a complete three dimensional network, the resulting material is composed of highly branched chains. In this case that part of the retardation spectrum arising from entanglement adjustment is enhanced³⁷ and most probably extends to much longer times than that of an equivalent molecular weight linear material. Therefore, since a lightly crosslinked rubber will differ little in behavior from a very high molecular weight branched material, except for the absence of permanent deformation (i.e., flow), the presence of the crosslinks will be responsible for the existence of many loss mechanisms not present in the precursor. The elimination of mechanisms with increasing crosslinking as described earlier will be relative to some maximum present in a nascent molecular network.

The dotted lines in Fig. 8 represent a decomposition of the spectrum of J into two groups of mechanisms by allowing an extrapolation of the spectrum derived from $J_e(F)\psi_x(t)$ to short times. The resulting fall from the maximum appears reasonable, but the ascending tendency of the other curve clearly indicates that such an extrapolation cannot be valid at times shorter than $\log \tau_r < -5$. A plateau to the left of the maximum would be predicted and such does not exist.²² This conclusion is in accord with the statement that $\log a_x$ does not represent a difference in molecular friction coefficient but a decrease in the number of

contributing retardation mechanisms. Although it appears not to, $\psi_x(t)$ actually changes shape as crosslinking increases; it does not actually shift on the time scale.

It can be seen in Fig. 8 that the apparent one-half logarithmic decade difference in the position of the F and J creep compliance curves (see Fig. 6) at short times, $\log t/a_T < -5$, is in reality largely a difference in the heights of the primary transition peaks in L and not a difference in friction coefficient which would imply a substantial difference in free volume in the two rubbers. Less than 1/3 of the difference can be accounted for by estimating the enhancement of peak heights arising from short time entanglement mechanisms or in other words mechanism overlap. The main reason for the smaller primary transition peak of J must be that in J the average molecular weight between crosslinks, M_c (5300), is smaller than M_e (6400). More long-time, entanglement and crosslink unencumbered, normal mode chain motions are present in the response of F simply because F contains longer chains between impediments.

CONCLUSIONS

The measurements of the shear creep compliance of the NR vulcanizates have been found to be in agreement with the elongational stress relaxation results of Chasset and Thirion.¹¹ Attainment of true mechanical equilibrium in air was not achieved and judged impossible before the intervention of thermal degradation. The molecular weight between crosslinks, M_c , has been proposed as a reduction variable. Application of the proposal leads to an extended reduced curve which may be used to estimate J_e for vulcanizates from limited creep data. The (23.5/76.5) SBR rubber system has been shown to exhibit, within a proportionality factor the same approach to equilibrium. The velocity of creep appears to be solely a function of the distance from equilibrium. A phenomenological picture of the effect of the degree of crosslinking on the viscoelastic behavior of elastomers has been presented. The principle effects of the crosslink density on the retardation spectrum are in the region of time scale where in an uncrosslinked polymer the retardation mechanisms observed are attributed to long-range coordinated motions that exist because of molecular entanglements. A priori, there appears to be no reason to invoke mechanisms besides the restrictive interaction of the chemical crosslinks on the response of the transient entanglement network.

It is pointed out that when the average molecular weight between crosslinks approaches that between entanglements the restrictive action extends to the primary softening transition.

ACKNOWLEDGMENTS

This work was supported by the National Aeronautics and Space Administration under Research Grant NsG 147-61. I wish to gratefully acknowledge the experimental assistance of Messrs. V. Michael O'Rourke and Solomon A. Nasser in carrying out the creep measurements, and of Mr. Louis Piasecki in obtaining the swelling values reported.

REFERENCES

1. Zapas, L. J., S. L. Shufler, and T. W. DeWitt, *J. Polymer Sci.* 18, 245 (1955).
2. Fletcher, W. P. and A. N. Gent, *Brit. J. Appl. Phys.* 8, 194 (1957).
3. Payne, A. R. in "Rheology of Elastomers," P. Mason and N. Wookey, Ed., Pergamon Press Ltd. London, 1958, p. 86.
4. Wood, L. A. and F. L. Roth, Proc. Fourth Rubber Technology Conference, London, England, May 1962. Paper No. 28, p. 328, Institution of the Rubber Industry, London 1963; *Rubber Chem. Technol.* 36, 611 (1963).
5. Roth, F. L., G. W. Bullman, and L. A. Wood, *J. Research Nat. Bur. Standards*, 69A, 347 (1965).
6. Kuhn, K. and O. Künzle, *Helv. Chim. Acta*, 30, 839 (1947).
7. Catsiff, E. and A. V. Tobolsky, "Viscoelastic Properties of Natural Rubber and GR-S Gum Vulcanizates," ONR Technical Report RLT-21, Dec. 18, 1956, (summarized in A. V. Tobolsky, "Properties and Structure of Polymers," John Wiley & Sons, Inc., New York, 1960).
8. Bueche, F., *J. Polymer Sci.*, 25, 305 (1957).
9. Gent, A. N., *J. Appl. Polymer Sci.* 6, 433 (1962).
10. Stratton, B. and J. D. Ferry, *J. Phys. Chem.* 67, 2781 (1963).
11. Chasset, R. and P. Thirion, "Proceedings of the International Conference on Non-Crystalline Solids," North-Holland Publishing Co., Amsterdam, 1965, p. 345.
12. Thirion, P. and R. Chasset, *Rev. gen. Caoutchouc*, 41, 271 (1964).
13. Ferry, J. D., R. G. Mancke, E. Maekawa, Y. Oyanagi, and R. A. Dickie, *J. Phys. Chem.* 68, 3414 (1964).
14. Flory, P. J. and J. Rehner, Jr., *J. Chem. Phys.* 11, 521 (1943); Flory, P. J., *Ibid.*, 18, 108 (1950).
15. Plazek, D. J., *Trans. Soc. Rheology* 7, 61 (1963).
16. Tobolsky, A. V. and R. D. Andrews, *J. Chem. Phys.*, 13, 3 (1945).
17. Mandelkern, L., *Chem. Rev.*, 56, 903 (1956).

18. Gent, A. N., J. Polymer Sci., 18, 321 (1955).
19. Bisschops, J., J. Polymer Sci., 12, 583 (1954).
20. Plazek, D. J. and J. D. Ferry, J. Phys. Chem., 60, 289 (1956).
21. Gent, A. N., J. Appl. Polymer Sci., 6, 442 (1962).
22. Ferry, J. D., "Viscoelastic Properties of Polymers," John Wiley and Sons Inc., New York, N. Y., 1961, Chapter 11.
23. Rivlin, R. S., Phil. Trans. A, 242, 173 (1949).
24. Thirion, P. and R. Chasset, Internal report, Institut Francais du Caoutchouc, No. 49 (1963).
25. Leaderman, H. in F. R. Eirich "Rheology", Vol. II, Academic Press, New York, 1958.
26. Flory, P. J., "Principles of Polymer Chemistry," Cornell University Press, Ithaca, N. Y. 1953, Chapter 11.
27. Tobolsky, A. V., D. W. Carlson, and N. Indictor, J. Polymer Sci., 54, 175 (1961).
28. Flory, P. J., J. Am. Chem. Soc. 78, 5222 (1956); Flory, P. J., C. A. J. Hoeve, and A. Ciferri, J. Polymer Sci., 34, 337 (1959).
29. Stern, D. M., Ph.D. Thesis, University of Wisconsin, 1957; Williams, M. L. and J. D. Ferry, J. Polymer Sci., 11, 169 (1953).
30. Wood, L. A. in "Synthetic Rubber," Ed. G. S. Whitby, John Wiley & Sons, Inc. New York, N. Y., 1954, Chapter 10.
31. Williams, M. L., R. F. Landel, and J. D. Ferry, J. Am. Chem. Soc. 77, 3701 (1955).
32. Bueche, A. M., J. Polymer Sci., 19, 297 (1956).
33. Mullins, L., J. Appl. Polymer Sci. 2, 1 (1959).
34. Plazek, D. J., J. Colloid Sci. 15, 50 (1960).
35. Markovitz, H., T. G. Fox, and J. D. Ferry, J. Phys. Chem. 66, 1567 (1962).
36. Maekawa, E., R. G. Mancke, and J. D. Ferry, J. Phys. Chem. 69, 2811 (1965).
37. Author, unpublished experiments.

LEGENDS FOR FIGURES

- Figure 1 The shear creep compliance, $J_p(t)$, cm^2/dyne , of natural rubber samples F and I plotted logarithmically against the time, sec. Temperatures of measurement indicated. Subscript p indicates amplitude adjustment for the theoretically predicted temperature dependence. Note difference in scales.
- Figure 2 Logarithmic plot of $J_p(t)$ against reduced time scale, t/a_T , for samples F, H, I, and J. a_T is the time scale shift factor required for temperature reduction. Reference temperature $T_0 = 30^\circ\text{C}$. Dashed lines represent shear creep compliances calculated from elongational stress relaxation measurements of Chasset and Thirion at an extension ratio, λ , equal to 1.5.
- Figure 3 Temperature reduced compliance curves for sample I and J presented as in Fig. 2, but with an expanded ordinate scale.
- Figure 4 Logarithmic plot of $J_x(t)$, the extended compliance curve resulting from reduction using M_c as a reduction variable, versus the logarithm of the reduced time, t/a_x . $J_p(t)$ curves of samples H, I, and J have been reduced to the reference sample F. The second approximation calculation of the retardation spectrum, L_2 , derived from $J_x(t)$ is also presented logarithmically.
- Figure 5 $\log a_x$ shown plotted against the logarithm of the apparent molecular weight between crosslinks, M_c , for the natural rubber, NR, and styrene-butadiene rubber, SBR series. Filled-in points from swelling measurements, this study; open points from ref. 11.
- Figure 6 Temperature reduced $\log J_p(t)$ curves of F and J extended to primary softening transition at shorter reduced times ($\log t/a_T$) using lower temperature measurements as indicated. Solid lines between $\log t/a_T$ of -1 and 5 from Fig. 2. Long dashed lines are appropriately positioned $\log J_x(t)$ curve. Short dashed lines indicate vertical position of lower temperature results on F as measured.

Figure 7 Logarithms of temperature shift factors a_T determined for samples F, H, and J as function of temperature. Line calculated from WLF equation.

Figure 8 Second approximation to retardation spectra for all samples presented logarithmically as a function of the logarithmic reduced retardation times; reference temperature, $T_0 = 30^\circ\text{C}$. Dashed line from Fig. 4. Dotted lines indicate a decomposition of the spectrum of J.

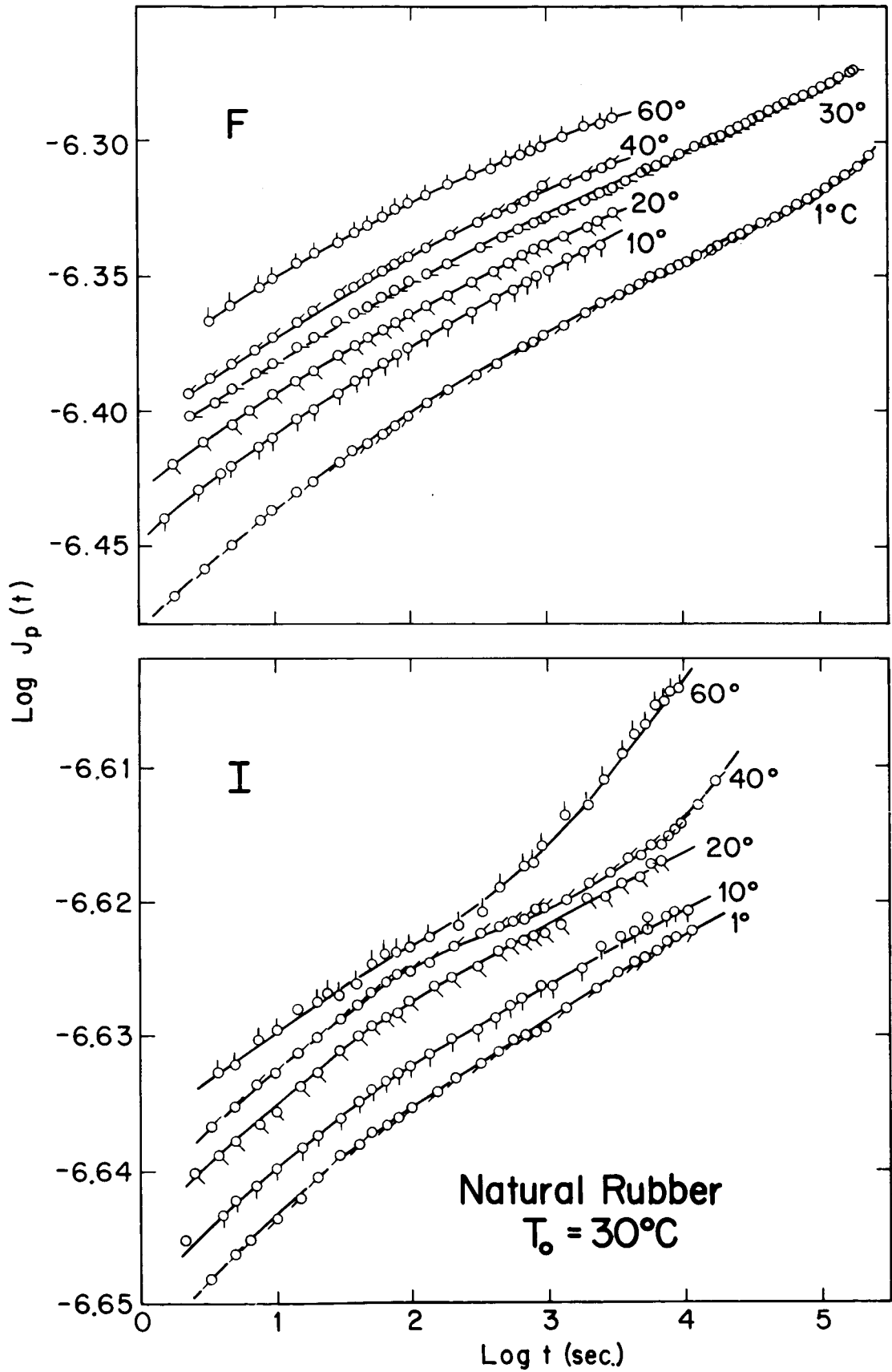


Figure 1

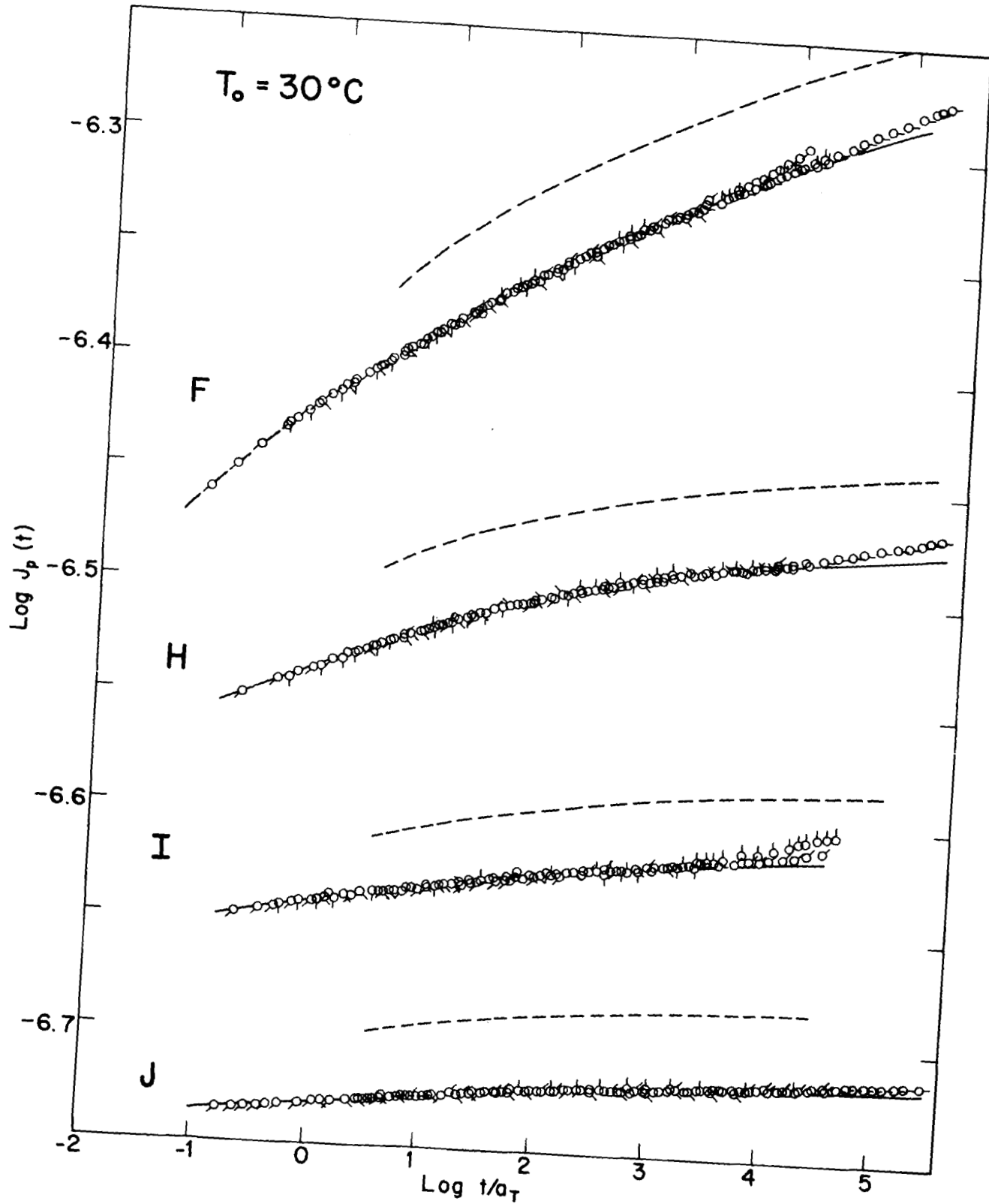


Figure 2

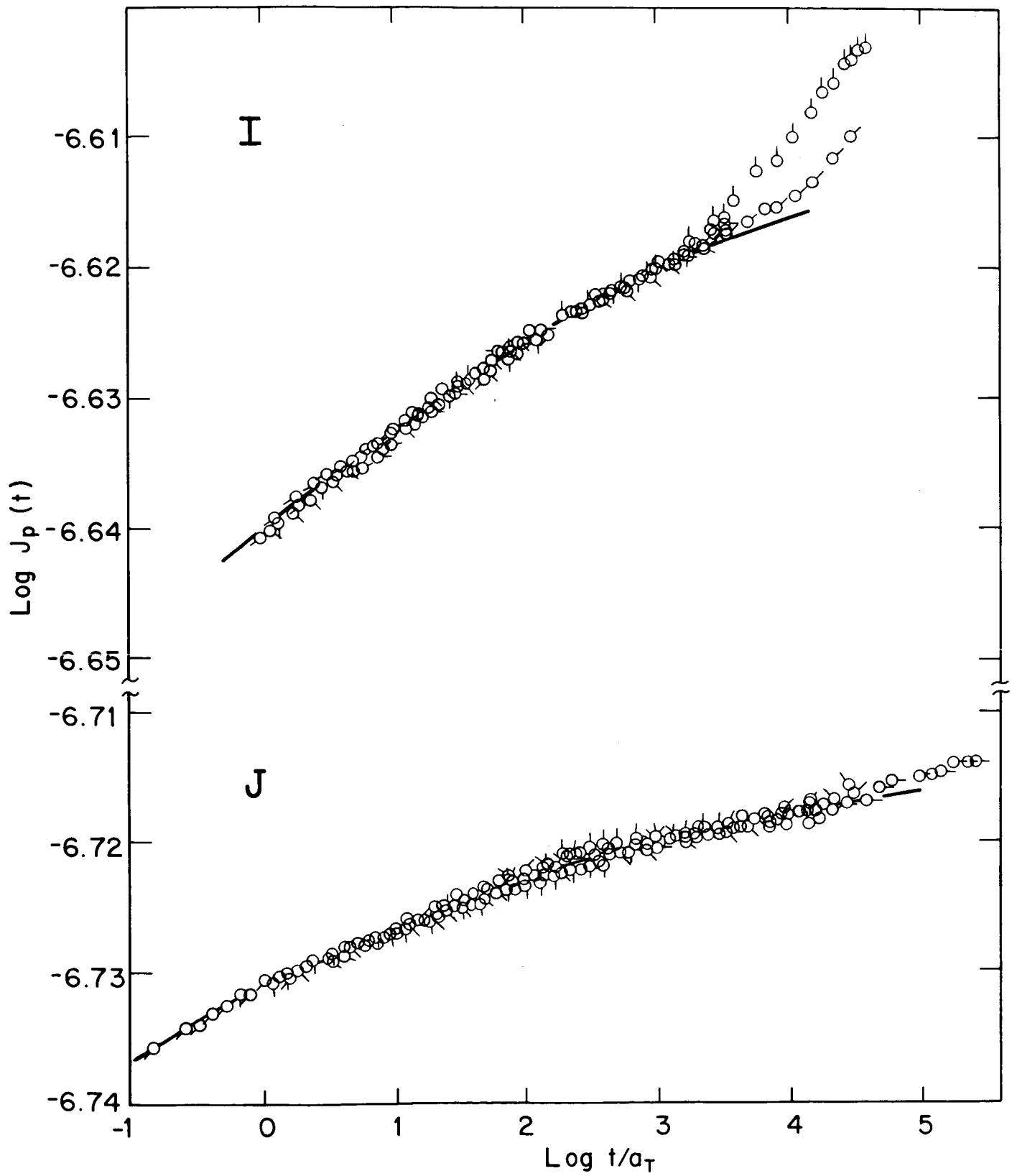


Figure 3

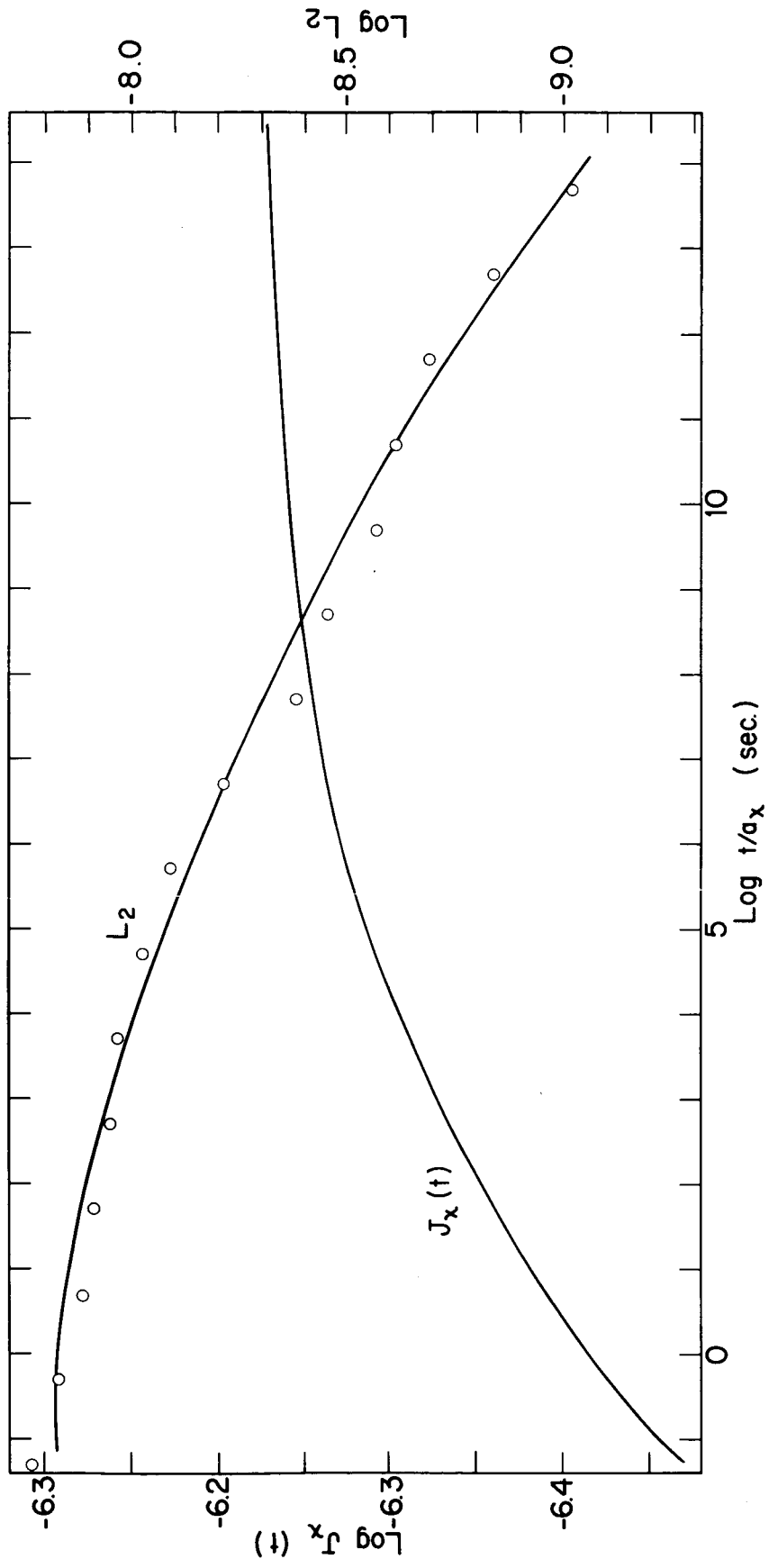


Figure 4

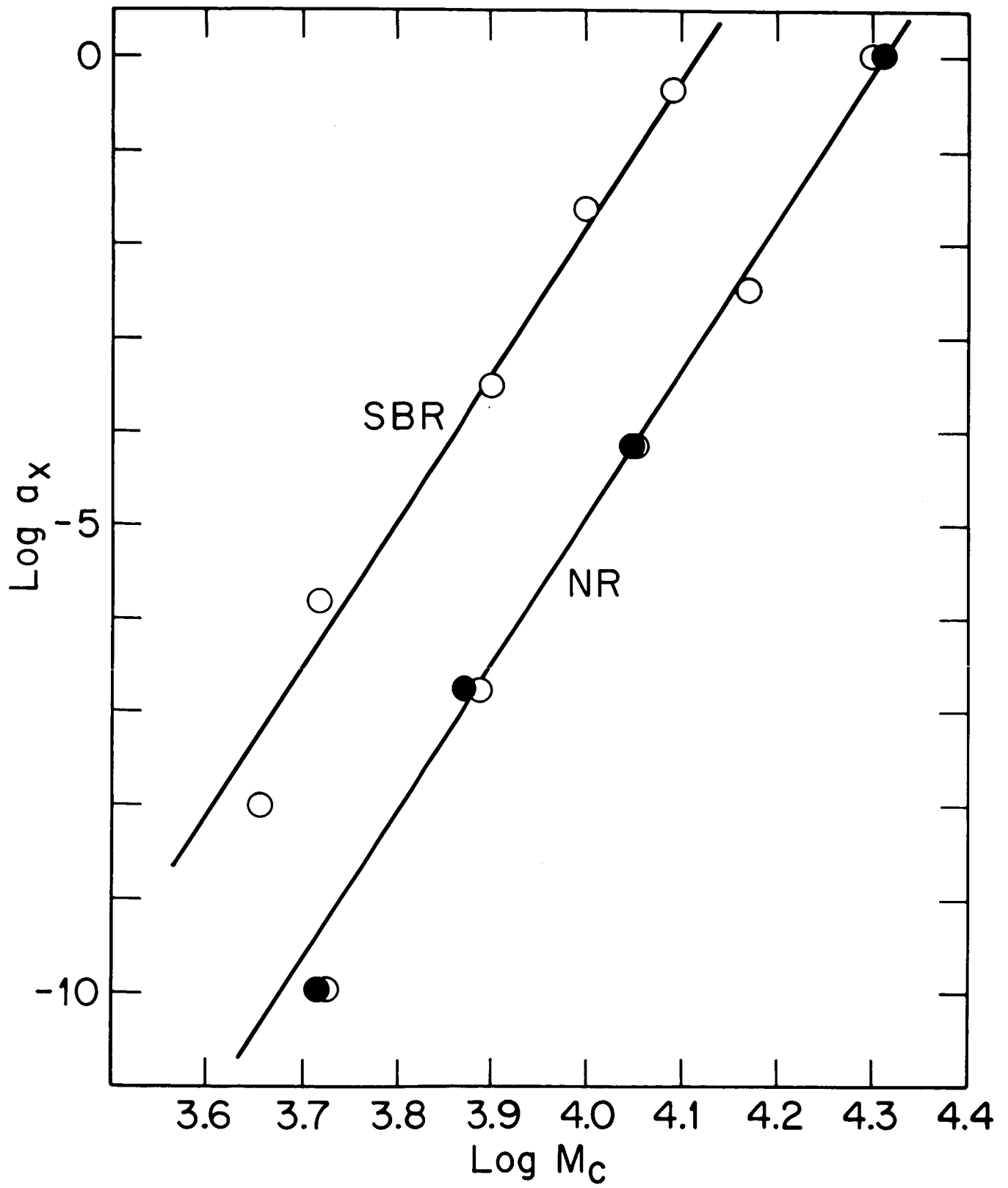


Figure 5

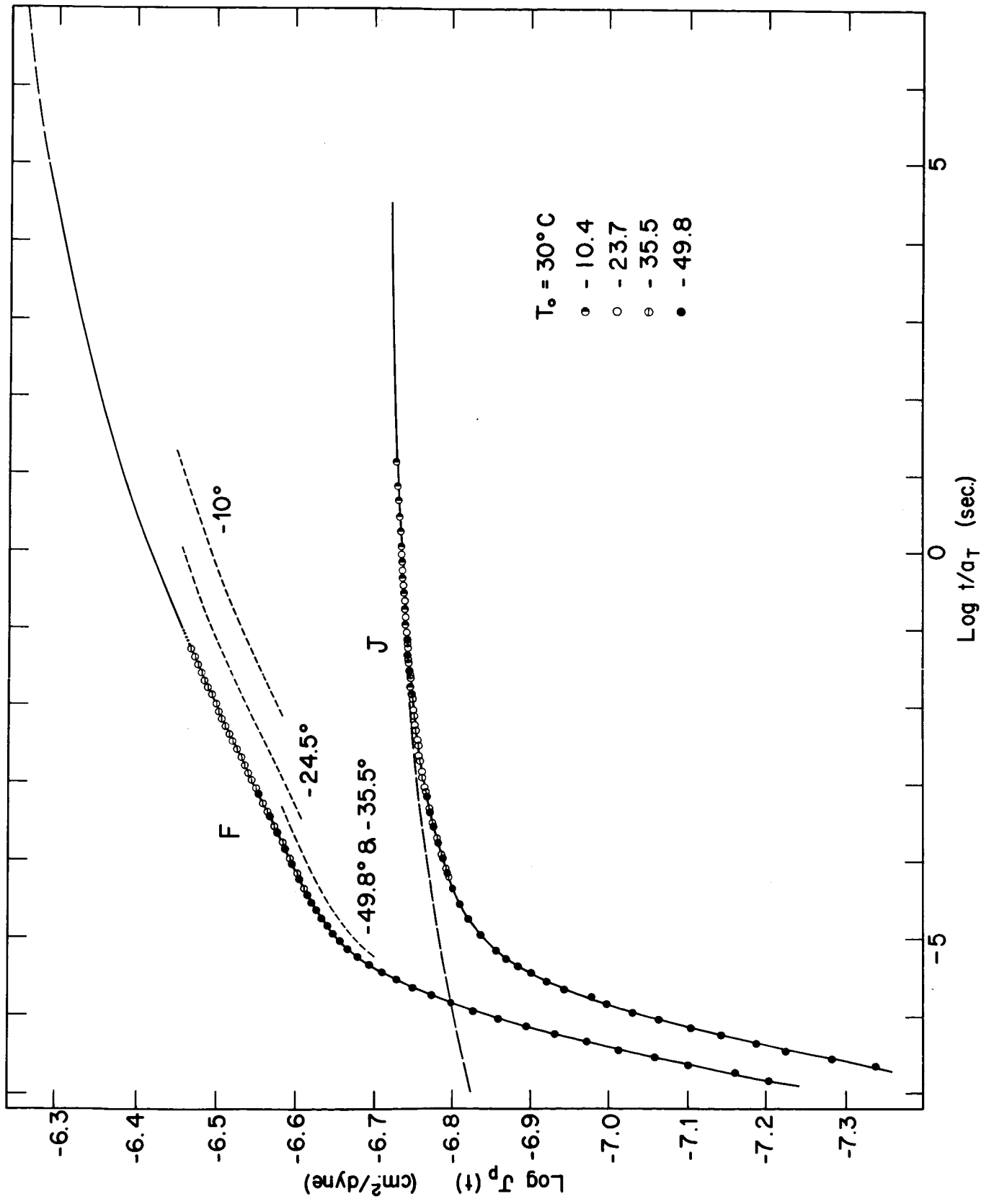


Figure 6

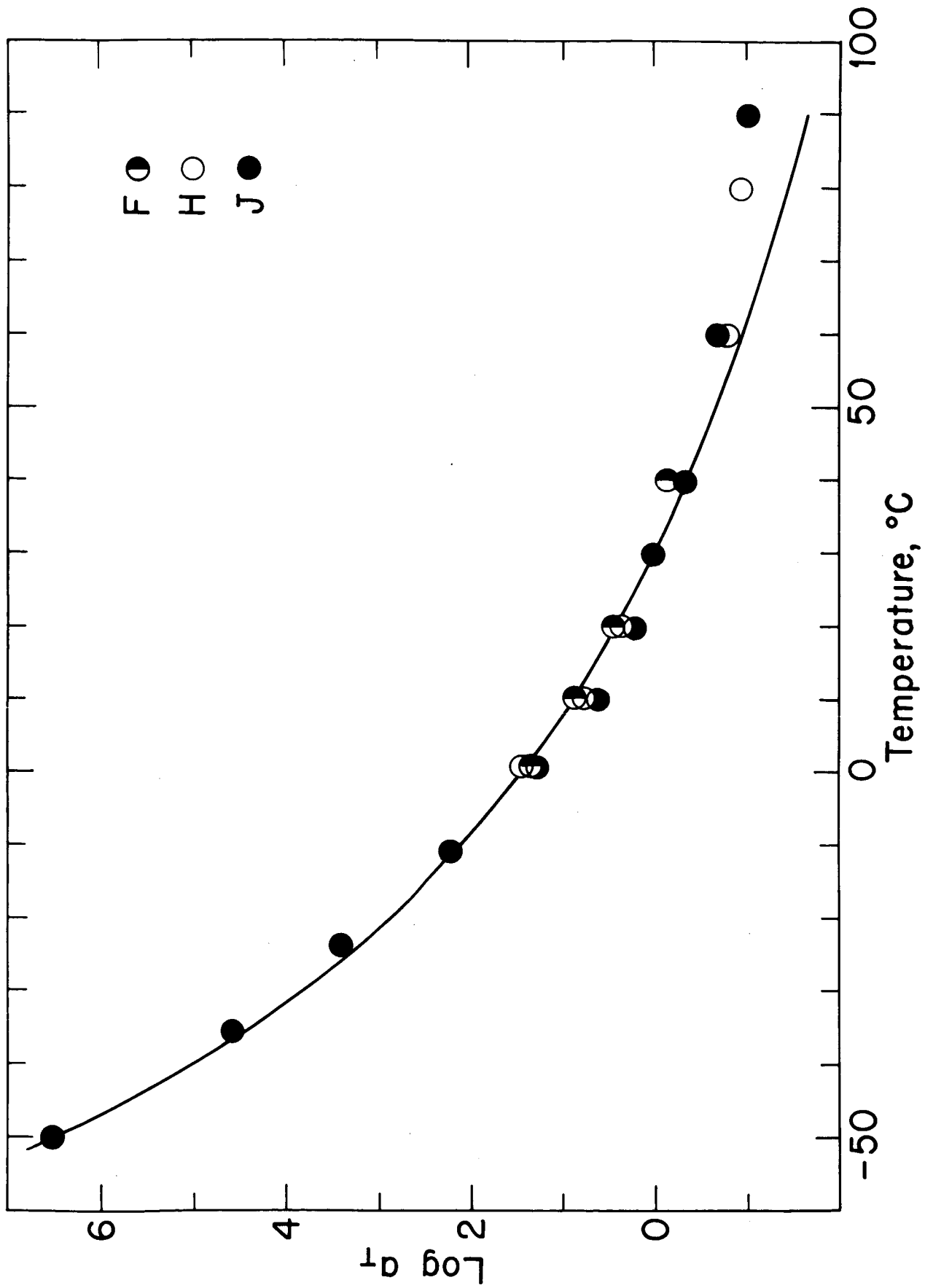


Figure 7

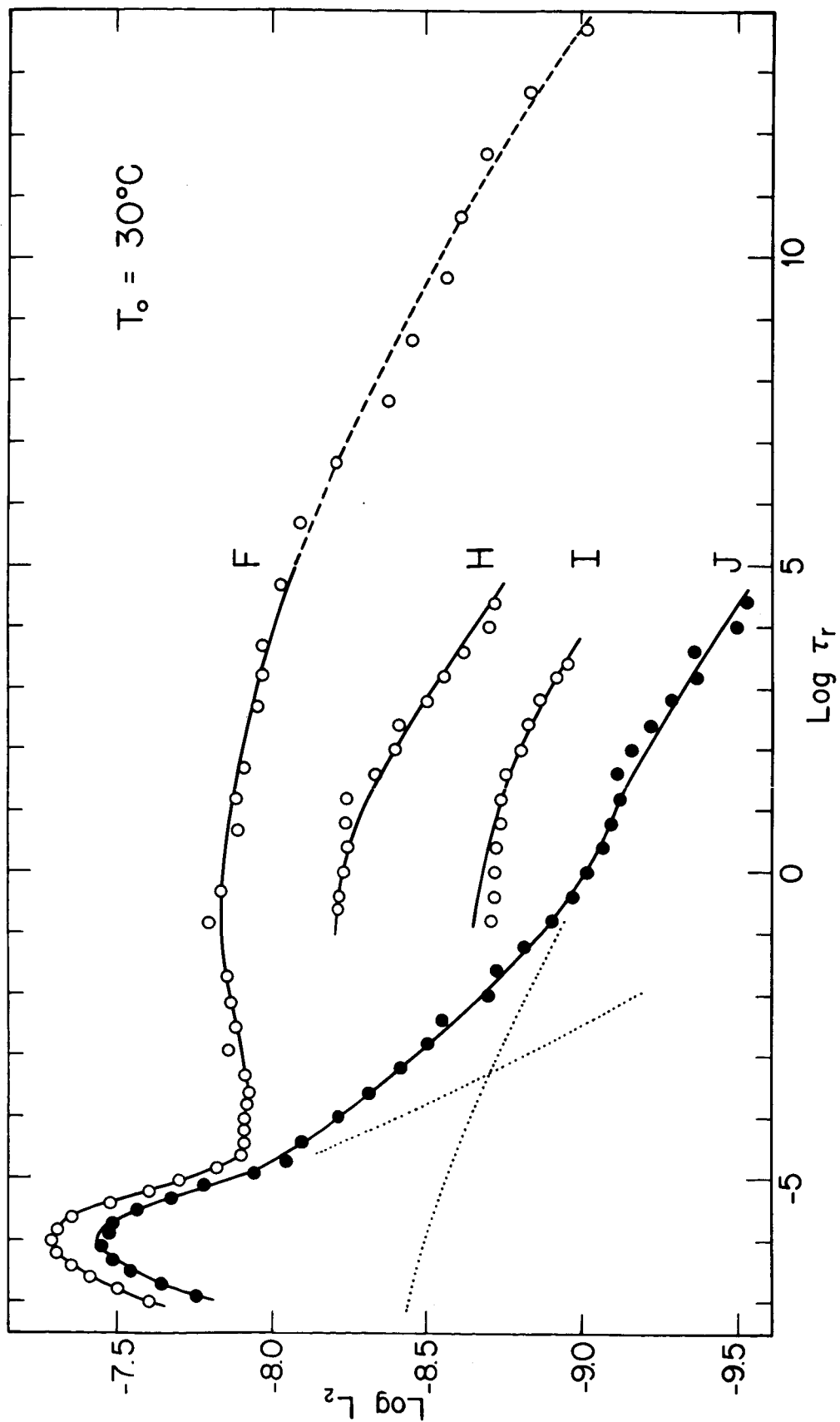


Figure 8